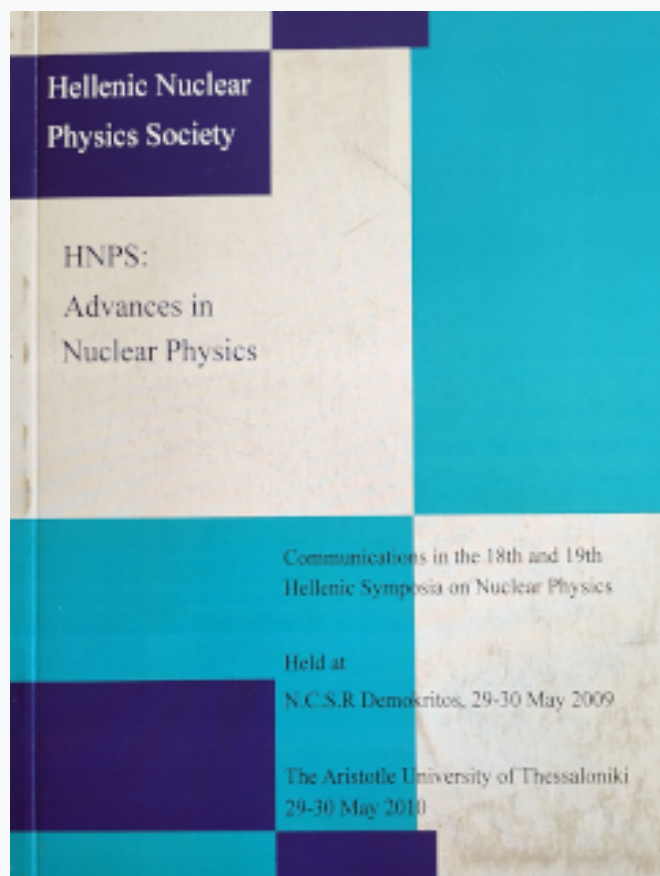


HNPS Advances in Nuclear Physics

Vol 18 (2010)

HNPS2010



To cite this article:

Tsakstara, V., Kosmas, T. S., & Sinatkas, J. (2019). Studying supernova neutrinos through nuclear structure calculations. *HNPS Advances in Nuclear Physics*, 18, 193–199. <https://doi.org/10.12681/hnps.2552>

Studying supernova neutrinos through nuclear structure calculations

V. Tsakstara ^a T.S. Kosmas ^a and J. Sinatkas ^b

^a*Theoretical Physics Section, University of Ioannina, GR 45110 Ioannina, Greece*

^b*Department of Informatics and Computer Technology, TEI of Western Macedonia, GR-52100 Kastoria, Greece*

Abstract

Differential and integrated cross section calculations are performed in the context of the quasi particle random phase approximation (QRPA) by utilizing realistic two-nucleon forces, for the $^{64,66}\text{Zn}$ isotopes, contents of the COBRA double beta decay detector. For these isotopes the response to supernova neutrinos is of current interest. The response of the ^{66}Zn isotope to the energy-spectra of supernova neutrinos is also explored by convoluting the original results for the differential cross sections by employing: (i) a two-parameter Fermi-Dirac (FD) and (ii) a Power-Law (PL) neutrino energy distribution. Such folded cross sections are useful in low-energy astrophysical-neutrino detection in underground terrestrial experiments.

Key words: Neutrino-nucleus reactions, Supernovae.

PACS: 23.20.Js, 23.40.-s, 25.30.-c, 24.10.-i.

1 Introduction

Terrestrial neutrino experiments and telescopes provide crucial information about the weak processes taking place in the interior of stars thanks to the fact that neutrinos are extremely sensitive probes for studying stellar evolution and astro-nuclear processes. They provide the main signal from distant stars since electromagnetic signals fail to reach the detectors. Recent measurements of solar neutrinos (KAMLAND, Borexino, etc.) have been used to test the standard solar model (SSM) while recent probes at SNO (SNO+ experiment) aim to measure low-flux solar neutrinos (pep and CNO-cycle neutrinos) to check the abundances of the solar core and clarify if the metallicity in the Sun is homogeneous [1,2].

Among the promising double beta decay detectors, the semiconductor detectors CdTe and CdZnTe, and also the TeO₂ are used in the COBRA and CUORE experiments at Gran Sasso [2,3]. In these materials, the Zn isotopes have large portion and an investigation of their potential use in low-energy neutrino detection (or neutrino cross sections measurements) has not yet been addressed. We mention that, the most abundant Te isotopes, ^{128,130}Te, of these experiments have been investigated in detail in Ref. [3]. It is the purpose of the present work to study the response of ^{64,66}Zn isotopes (which have big abundances on the natural Zn) to the low-energy neutrino spectra through detailed state-by-state cross-section calculations of their neutral current reactions with neutrinos and anti-neutrinos.

194

It is worth mentioning that the COBRA experiment has recently been funded and an investigation of the response of its isotopes as supernova neutrino detectors but also, in general, as detectors of low-energy astrophysical and laboratory neutrinos is of current interest. In this work we study the nuclear response of the COBRA detector isotopes to the supernova neutrino energy spectra. We focus on the ^{64,66}Zn isotopes which have big abundances on the natural Zn of the matter of the CdZnTe detector [2].

2 The Structure of the ^{64,66}Zn isotopes

In the present paper, we present only original results for the cross sections of (anti)neutrino reactions with the isotopes ⁶⁴Zn and ⁶⁶Zn obtained within the context of the quasi-particle RPA of pp-nn type. We study the neutral current neutrino-nucleus reactions

$$\nu_l + {}^{64,66}Zn \rightarrow {}^{64,66}Zn^* + \nu_l', \quad (1)$$

$$\tilde{\nu}_l + {}^{64,66}Zn \rightarrow {}^{64,66}Zn^* + \tilde{\nu}_l', \quad (2)$$

where $\ell = e, \mu, \tau$ [4]. In the first stage, we determine the model parameters describing the nuclear structure of ⁶⁴Zn and ⁶⁶Zn as follows.

2.1 Determination of the model parameters

The final wavefunctions $|J_f^\pi\rangle$ of the nuclei ⁶⁴Zn or ⁶⁶Zn entering the description of the interactions of Eqs. (1) and (2), are very important for the cross section calculations. Their reliability has been checked by the reproduction of the low-lying excitation spectrum ($\omega \preceq 4$ MeV) of the isotopes ^{64,66}Zn which is induced by the neutrinos(antineutrinos) of the reaction. We used as model

Table 1

Parameters determining the pairing interaction for protons, g_{pair}^p , and neutrons g_{pair}^n . They reproduce rather well the corresponding (for each isotope) empirical energy gaps $\Delta_{p,n}^{exp}$ listed also in this table (the values of the harmonic oscillator size parameter b used for $^{64,66}Zn$ isotopes are also shown).

195

| | b (fm) | g_{pair}^n | g_{pair}^p | S_n | S_p | Δ_p^{exp} | Δ_p^{th} | Δ_n^{exp} | Δ_n^{th} |
|-----------|--------|--------------|--------------|--------|-------|------------------|-----------------|------------------|-----------------|
| ^{64}Zn | 2.034 | 0.933 | 0.823 | 11.862 | 7.713 | 1.372 | 1.368 | 1.658 | 1.668 |
| ^{66}Zn | 2.043 | 0.964 | 0.839 | 11.059 | 8.925 | 1.282 | 1.288 | 1.772 | 1.772 |

Table 2

Renormalization parameters for the particle-hole, g_{ph} , and particle-particle, g_{pp} , channel of the residual interaction for ^{64}Zn and ^{66}Zn isotopes (different for each multipolarity). They have been determined so as the low-lying excitation spectrum of each isotope ($\omega \preceq 4$ MeV) to be reproduced.

| J^+ | ^{64}Zn | | ^{66}Zn | | J^- | ^{64}Zn | | ^{66}Zn | |
|-------|-----------|----------|-----------|----------|-------|-----------|----------|-----------|----------|
| | g_{pp} | g_{ph} | g_{pp} | g_{ph} | | g_{pp} | g_{ph} | g_{pp} | g_{ph} |
| 0^+ | 0.765 | 0.369 | 0.765 | 0.354 | 0^- | 0.940 | 1.123 | 1.000 | 1.000 |
| 1^+ | 1.260 | 1.287 | 0.880 | 1.120 | 1^- | 0.810 | 0.390 | 0.510 | 0.440 |
| 2^+ | 1.026 | 0.483 | 1.026 | 0.480 | 2^- | 1.220 | 1.190 | 1.250 | 1.300 |
| 3^+ | 1.170 | 1.170 | 1.000 | 1.000 | 3^- | 0.910 | 0.620 | 0.829 | 0.700 |
| 4^+ | 1.010 | 0.610 | 0.900 | 0.610 | 4^- | 1.150 | 1.250 | 1.000 | 1.000 |
| 5^+ | 1.180 | 0.400 | 1.000 | 1.000 | 5^- | 0.980 | 1.020 | 0.941 | 0.900 |
| 6^+ | 1.030 | 1.000 | 1.200 | 1.003 | 6^- | 1.220 | 1.230 | 0.890 | 0.900 |
| 7^+ | 1.080 | 1.060 | 0.950 | 0.950 | 7^- | 1.070 | 1.090 | 0.950 | 0.950 |
| 8^+ | 0.895 | 0.880 | 0.950 | 0.950 | 8^- | 1.230 | 1.220 | 0.900 | 0.900 |

space the 14 lower energy levels up to $N = 4\hbar\omega$ with core the ^{16}O , the major shells with 2, 3, 4 ($\hbar\omega$).

In Tables 1 and 2, we tabulate the values of the parameters used for the construction of the nuclear states of the isotopes $^{64,66}Zn$: the initial (ground) state, which has been constructed by the BCS method and the final excited states which have been constructed within the QRPA method [4,5].

The nuclear ground state of each isotope has been constructed by solving the BCS equations using as single particle energies those determined by a Coulomb corrected Woods-Saxon potential which includes also spin-orbit part and it is given by the equation

$$V(r) = V_{central}(r) - V_{so}r_0^2 \frac{1}{r} \frac{\partial V_{central}(r)}{\partial r} (\vec{L} \cdot \vec{S}) + \frac{1 + \tau_3}{2} V_C(r), \quad (3)$$

As central potential, $V_{central}(r)$, as usually, we used the Woods-Saxon potential, which is given by the expression

$$V_{central}(r) = -\frac{V_0}{1 + \exp[\frac{r-R}{\alpha}]} . \quad (4)$$

The correction Coulomb for protons is produced by an homogeneously charged sphere of radius R_c , given as

$$V_C = \begin{cases} \frac{(Z-1)e^2}{2R_0} \left[3 - \left(\frac{r}{R_c} \right) \right], & \text{for } r \leq R_c \\ \frac{(Z-1)e^2}{2r}, & \text{for } r > R_c \end{cases} \quad (5)$$

The pairing strength parameters for proton pairs, g_{pair}^p , and neutron pairs g_{pair}^n have been adjusted so as the semi-empirical pairing gaps denoted as $\Delta_{p,n}^{exp}$, to be reproduced. From Table 1 it is obvious that, there is a very good agreement between the empirical energy gaps for neutrons, Δ_n^{exp} , and for protons, Δ_p^{exp} , with the corresponding theoretical lowest quasiparticle energy which had been determined by the separation energies for protons, S_p , and for neutrons, S_n , by using the equations (known as three point semi-empirical formulae)

$$\Delta_n^{exp} = -\frac{1}{4} \{ S_n[(N-1), Z] - 2S_n[(N, Z)] + S_n[(N+1), Z] \} , \quad (6)$$

$$\Delta_p^{exp} = -\frac{1}{4} \{ S_p[(N, Z-1)] - 2S_p[(N, Z)] + S_p[(N, Z+1)] \} . \quad (7)$$

In Table 2, we tabulate the values of the parameters used in the context of the QRPA for the determination of the wave function and energies of the final nuclear states $|J^\pi\rangle$ ($J^\pi \preceq 8^\pm$, for the isotopes ^{64}Zn and ^{66}Zn). Specifically, for the construction of the QRPA matrices \mathcal{A} and \mathcal{B} , the renormalization parameters for the particle-hole, g_{ph} , and particle-particle, g_{pp} , channel of the residual interaction for ^{64}Zn and ^{66}Zn isotopes, have been determined separately for each multipole $|J_m^\pi\rangle$, so as the low-lying QRPA excitations ($E_\delta \preceq 4$ MeV) to fit the corresponding experimental spectrum.

After the determination of the the pairing parameters, g_{pair}^p , and neutrons g_{pair}^n and the parameters particle-hole, g_{ph} , and particle-particle, g_{pp} , the resulting energy spectrum is compared with the corresponding experimental of ^{66}Zn , in Fig. 1. As can been seen, with a few exceptions the agreement is good.

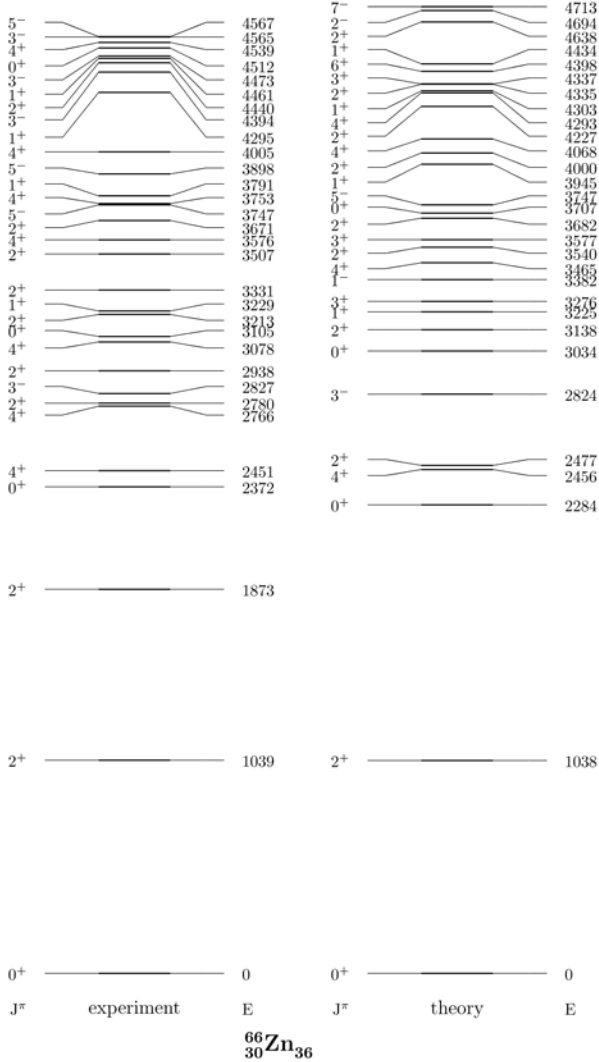


Fig. 1. Experimental and theoretical spectrum of the ^{66}Zn isotope.

3 Results and discussion

The calculational procedure of this work was carried out with the following steps. In the first step, the original results for the double differential cross section $d^2\sigma/d\Omega d\epsilon_f$ [3,4], were obtained for both nuclear isotopes, $^{64,66}\text{Zn}$. Figure 2, shows the double differential cross section as a function of the excitation energy ω of the nucleus and the scattering angle θ of the outgoing lepton, for ^{66}Zn . For all the excitation energies ω in the range $0 < \omega < 25 - 30$ MeV, the cross section is clearly backward peaked ($\theta \approx 180$), a result that comes from the contribution of the transverse term of the operator which describes the interaction of the neutrino- $^{64,66}\text{Zn}$. This behavior was also found the $^{128,130}\text{Te}$ for neutral-current reactions in this energy range [3].

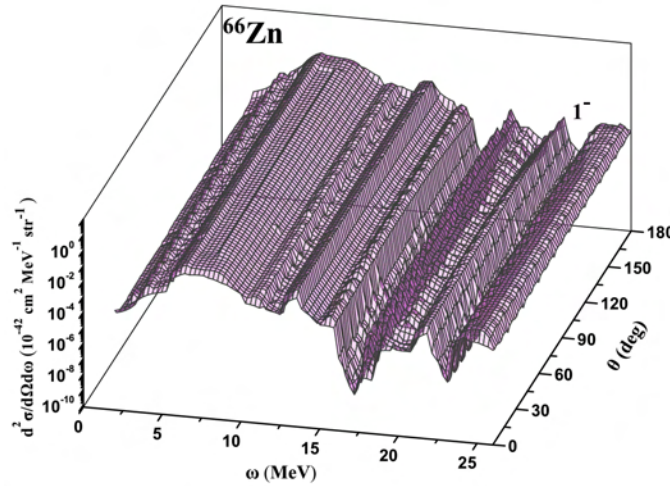


Fig. 2. The double differential cross section, $d^2\sigma/d\Omega d\omega$ as function of the excitation energy ω of the nucleus and the scattering angle θ of the outgoing lepton, for ^{66}Zn . The incoming neutrino energy is $\varepsilon_\nu = 40$ MeV. The curves correspond to the principal multipolarity $J^\pi = 1^-$.

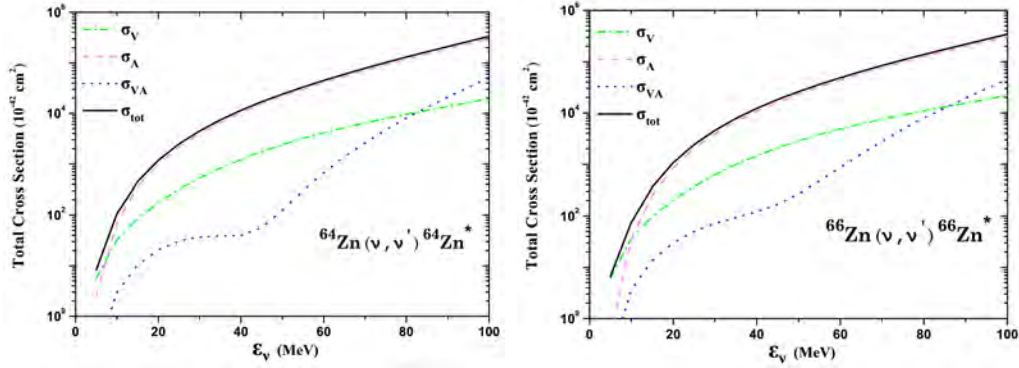


Fig. 3. Total cross sections σ_{tot} for the reaction $^{64}\text{Zn}(\nu, \nu')^{64}\text{Zn}^*$ (left) and for $^{66}\text{Zn}(\nu, \nu')^{66}\text{Zn}^*$ (right), respectively. The individual contributions of the polar-vector σ_V , axial-vector σ_A and of the interference term σ_{VA} are also illustrated.

In the final step of our calculations we studied total cross sections for the reactions of Eqs. (1) and (2). In Fig. 3, we plot the total cross section σ_{tot} (in logarithmic and linear scale) of the reactions $^{64,66}\text{Zn}(\nu, \nu')^{64,66}\text{Zn}^*$ as a function of the incoming neutrino energy ε_ν . For each reaction, the individual polar-vector, σ_V , and axial-vector, σ_A , parts as well as the interference term σ_{VA} are also illustrated.

By comparing the corresponding curves in the two Zn isotopes, we see that, there is a qualitative and quantitative similarity of the cross sections for ^{64}Zn and ^{66}Zn in all plots of Fig. 3, except a slight quantitative difference between the curves of the interference term σ_{VA} . For neutrino energies $\varepsilon_\nu \lesssim 5 - 8$ MeV, the polar-vector contribution σ_V dominates, while for large energies the axial-vector cross section σ_A is approximately equal to the total cross section

4 Summary and Conclusions

In the present work, we used the microscopic approach of the pp-nn quasi-particle QRPA to evaluate cross sections for the neutral current reactions $^{64}Zn(\nu, \nu')^{64}Zn^*$ and $^{66}Zn(\tilde{\nu}, \tilde{\nu}')^{66}Zn^*$. The Zn isotopes are main contents of the materials of the COBRA double-beta decay detector.

We started from double differential cross sections $d^2\sigma/d\Omega d\omega$, calculated (state-by-state) with the QRPA and, subsequently we obtained integrated $d\sigma/d\omega(\omega)$ and total σ_{tot} ones. These cross sections may be folded with the neutrino-energy distributions of specific neutrino sources to which the nuclear response is of current interest. The present results show that $^{64,66}Zn$ present rich responses in the excitation energy range $\omega \leq 20$ MeV (including transitions to bound states), relevant for solar neutrinos and geo-neutrinos but also for the low- and intermediate-energy supernova neutrinos. These inelastic neutrino-nucleus cross sections are suitable for use in astrophysical neutrino (including supernova neutrinos) simulations utilized in order to interpret neutrino oscillations, neutrino properties and supernova explosion mechanisms.

5 Acknowledgments

This research was supported by the ΠΙΕΝΕΔ No 03ΕΔ807 project of the General Secretariat for Research and Technology of the Hellenic Ministry of Development.

References

- [1] H. Ejiri, J. Engel, R. Hazama, P. Krastev, N. Kudomi, and R.G.H. Robertson, *Phys. Rev. Lett.* **85** (2000), 2917.
- [2] K. Zuber, *Phys. Lett. B* **519** (2001), 1–7; *Prog. Part. Nucl. Phys.* **57** (2006), 235–240.
- [3] V. Tsakstara and T.S. Kosmas, *Phys. Rev. C* (2011), in press.
- [4] V. Tsakstara, T.S. Kosmas, and J. Sinatkas, *Prog. Part. Nucl. Phys.* (2011), in press.
- [5] V.C. Chasioti and T.S. Kosmas, *Nucl. Phys. A* **829** (2009), 234–252.